Development and Application of OPC Simulation in OLED Panel Design

Huomei Hua, Huangyao Wu*, Liu Wang*, Jin Chen*, Linwen Kong**, Haiyan Zhang***
Xingyao Zhou, Hui Zhang*, Jianxing Li*, Zhiqiang Xia*, Kang Yang*, Bong-Geum LEE**

***Tianma Microelectronics Co., Ltd., Xiamen, China**
****Empyrean Technology Co., Ltd, Beijing, China**

Abstract

With the developments of OLED technologies, numerous tendencies are usually proposed, such as low-temperature polycrystalline silicon (LTPO), narrower bezel, higher PPI, higher brightness, and the usage of photo masks as few as possible. Meanwhile, the design of complex pixel circuits will become a bottleneck in the limited space for the achievement of high PPI and few mask simultaneously. However, it is also difficult to acquire the line width and space, which is close to the limit of the exposure machine as well. With these difficulties into consideration, in this paper, we provide a novel approach to solve the unique problems of reflection introduced by the stacking layers in backplate(BP) by improving the simulation accuracy of optical proximity correction(OPC), which does not exist in chip lithographic. With the help of this method, we can avoid deviation and yield loss by mask revision, which is due to in pixel circuits' open and shorts. Based on these result, we believe that this OPC simulation method will provide a more efficient and accurate technical solution for high PPI products (i.e., WQHD) in future, as well as AR/VR products.

Author Keywords

High PPI, Narrower bezel, LTPO, OPC, Pixel design

1. Introduction

According to Omdia's new market analysis, it is expected that by 2031, the shipment volume of mixed oxide low-temperature polycrystalline silicon (LTPO) OLED display panels for smartphones will increase to 520 million pieces. During this period, the market share of LTPO OLED display panels in smartphone OLED display panel shipments is expected to reach 52.0%. In order to improve the performance of OLED products such as image sticking and Flicker,8 TFT devices, 5 groups of Scan signals, and more than 3 reference signals are set in the pixel. This resulted in the reduction of line distance and space from the original 2.5 um to 1.8 um, which is close to the exposure limit.

As shown in Figure1, due to the optical proximity effect caused by the interference and diffraction of lights between close structures on the mask, the pattern on the photoresist is inconsistent with the pattern of the photo mask. [1-2]

If these deviations are not corrected, they will cause the design graphics to be inconsistent with the requirements, leading to changes in circuit performance, yield loss, and even mask revision. To deal with this problem, we can compensate it by introducing the graphical deviation to the mask, which is called optical proximity correction technology. [3-5]

The traditional optical proximity correction（rule-based OPC correction）is based on past experience to correct the graph, which has the following problems:

1. Cannot make correct compensation for new graphics.

2. Cannot make the correct compensation for different density.

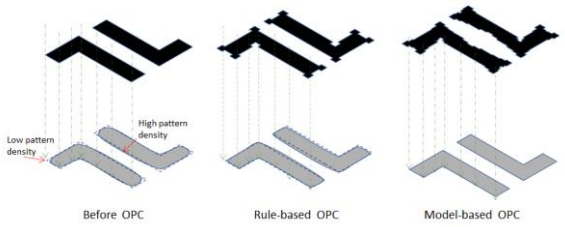

Figure 1. Rule-based and model-based OPC

As computing technology continues to advance，we can build optical and big data models of corrected graphics. The computer could simulate the lithographic deviation and automatically correct it. This tech called model-based OPC.

This OPC technology has been widely used in the IC industry. According to the Rayleigh Criterion, $CD = k1 * \frac{\lambda}{NA}$, resolution is related with K_1 factor, wave length λ and exposure machine numerical aperture (NA).[6] As shown in Figure2, the resolution of IC KrF exposure machine is about 120nm. So in the range from 250nm to 130nm，IC use rule-based OPC. However, below 130nm, the critical dimension becomes so close to the resolution of the exposure machine that ICs should use model-based OPC.

OLED panel design will go through the same process. The resolution of exposure machine is about 1.5um，and rule-based OPC used in OLED designs is no longer sufficient for production. So if we need better performance, model-based OPC is necessary in OLED design.

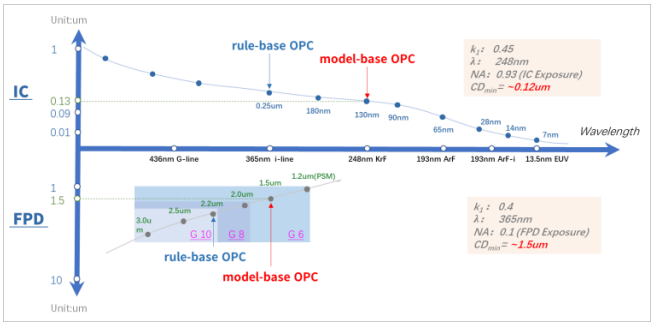

Figure 2. Application of OPC in IC and FPD industry

However, the lithographic of the OLED is more complex than that of IC. The inorganic layer flattening process is widely used in IC manufacturing but not used in the panel display industry. The substrate stacks will cause non-uniform photoresist thickness. The graphic contour will be bigger at the edge of the substrate stacks. And the reflected light from the substrate increases the exposure luminance resulting in a smaller contour. There are many factors influencing each other in the OLED panel lithographic compensation. So the model-based OPC of the panel needs a lot of improvement work about topography model compared with IC.

ISSN 0097-996X/25/5603-2248-$1.00 © 2025

2. Construction and calibration of OLED OPC model

2.1 The mechanism of Optical Proximity Correction

OPC simulator constructs the lithography process and establishes the OPC model. And then guides the layout correction. One of the most important modules of lithography simulation is the aerial image of the lithography system. According to the optical principle, accurate imaging models are constructed by mathematical modeling methods. The aerial image calculation model is Hopkins vector model.

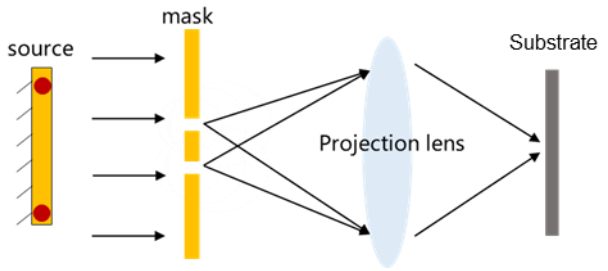

Figure 3. Lithographic imaging

As shown in **Figure 3**,the parallel light emitted by the light source arrive the mask. The resulting image is projected onto the substrate through projection lens.

In addition, the lighting system uses a partial coherence factor (δ) to characterize the shape of the light source. The projection optical system will transmit the mask information to the substrate in the form of low-pass filtering in the frequency domain to form the mask Aerial image.

The formula of Hopkins vector model for computing space image:[6]

$$I(x_i, y_i) = \iint TCC_v(f', g', f'', g'')O(f', g')O^*(f'', g'') \cdot \exp[-i2\Pi(f' - f'')x_i - i2\Pi(g' - g'')y_i]df'df''dg'dg'' \quad (1)$$

The TCCv function is called the cross-coefficient or transmission cross-coefficient (TCC) of the optical system. The TCC function describes the interaction between the imaging system and the light source. For a definite lithography system, the TCC function is fixed. In the photolithographic imaging simulation, the TCC function only needs to be calculated once for the definite light source and the projection imaging system. (x_i,y_i) represents spatial domain coordinates; (f ',g ') and (f ",g ") represent the spectral coordinates of the mask; O(f,g) is the mask diffraction spectrum distribution; O(f,g)=FT(M), FT(·) is the Fourier transform, and the superscript "*" indicates complex conjugation. The TCC function has the following form:

$$TCC_v = \iint S(f_s, g_s)\mathrm{T}(f' + f_s, g' + g_s) \cdot H(f' + f_s, g' + g_s) \cdot \mathbf{J} \times T^*(f'' + f_s, g'' + g_s) \times H^*(f'' + f_s, g'' + g_s) \cdot \mathbf{J}^* df_s dg_s \quad (2)$$

S(f_s, g_s) represents the light source, the normalized result of the light intensity distribution of the light source; (f_s, g_s) represents pupil plane coordinates; (f, g) is the coordinates of the mask diffraction spectrum; H(f_s+f, g_s+g) is the frequency response function of optical system. J=[J_x, J_y] represents the Jones vector of the illumination polarization state; T represents the electric field transformation matrix at the exit pupil, and the T function is generally represented by a 3*2 matrix, the six elements of which represent the T function values in different directions: [7]

$$T = \begin{pmatrix} T_{xx} & T_{xy} \\ T_{yx} & T_{yy} \\ T_{zx} & T_{zy} \end{pmatrix} \quad (3)$$

2.2 Data collection and experimental verification

An optical model requires some key parameters of the exposure machine and material, such as the light source file, the numerical aperture，the N/K value，thickness of the film material and photoresist, as shown in Table 1 to 3.

Table 1. Exposure parameters

Layer Name	Exposure parameters		
	Exposure NA	sigma_in	sigma_out
A	0.11	0.578	0.86
B	0.11	0.414	0.88

Table 2. PR parameters

Layer Name	PR parameters		
	PR thickness	PR N value	PR k value
A	1.5	1.63542	0.00305
B	1.5	1.63542	0.00305

Table 3. Inorganic layer parameters

Inorganic layer	layer thickness	N value	K value
A	5000Å	1.7	4.09
B	4000Å	1.9793	3.87

An optical topography model has been established according to the unique process issues of the panel, which is shown in Figure 4. It is assumed that Film1 is an oxide film layer and Film2 is a metal layer. Considering the three structures in the figure, the Model A which does not has Film1 and Film2 in substrate, Model B has Film1 and Film2 in substrate, and model C only has Film2 in substrate. Topography Model = Model A + Model B + Model C.

The issue of reflection and non-uniformity of photoresist caused by substrate stacks is solved by establishing three OPC models respectively.The heights and materials of the substrates being diff erent, the aerial imaging planes of the three structures vary.

So the topography model needs to be debugged based on actual substrate stacks. The topography model is still applicable when the substrate stacks is more complex. We need to establish more models to match it.

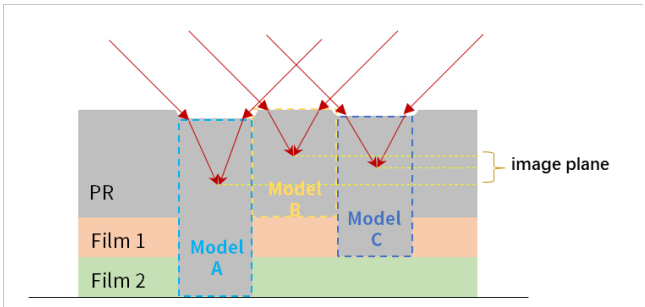

Figure 4. Topography model

1.3 Establish mathematical big data model

During the development process, a series of chemical reactions will occur, causing deviations in the prediction. Therefore, it is necessary to establish a photoresist model on the basis of the optical model (mathematical model). We need to collect more actual exposure data, build higher-order equations with large amounts of data. As Equations (4) and (5):

$$Shift_x = a_0 + a_1 x + a_2 x^2 + a_3 x^3 + \cdots + a_n x^n$$

$$Shift_y = b_0 + b_1 y + b_2 y^2 + b_3 y^3 + \cdots + b_n y^n \quad (4)$$

$$\textbf{Step I: } (Shift_x, Shift_y)\ (x_n, y_n) \Rightarrow \textbf{Step II: } (a_n, b_n)\ F(Shift_x, Shift_y)\ (x_n', y_n') \Rightarrow \textbf{Step III: } f(x), f(y) \quad (5)$$

As shown in Figure 5, a series of test keys are designed according to the design rule. They mainly consider CD range, substrate type, pitch range, and realistic panel graphics. Figure 6 shows the SEM image data of test keys after exposure. Such data are collected, higher-order equations are fitted, and models are calibrated. Finally, the model-based OPC for OLED panel is formed by optical topography model and mathematical model.

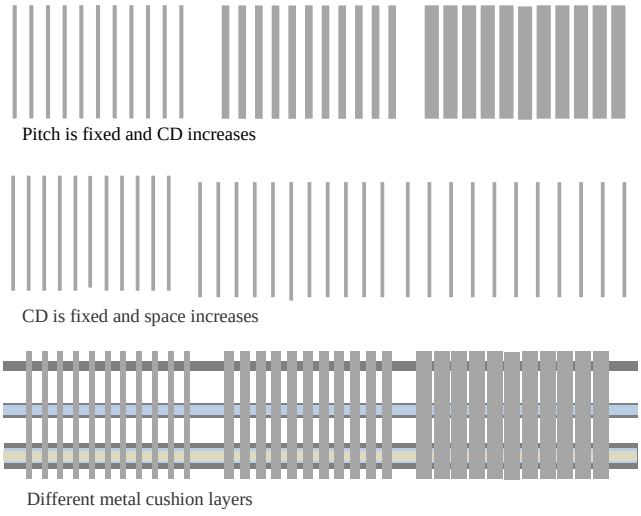

Figure 5. Design of different stacked test keys

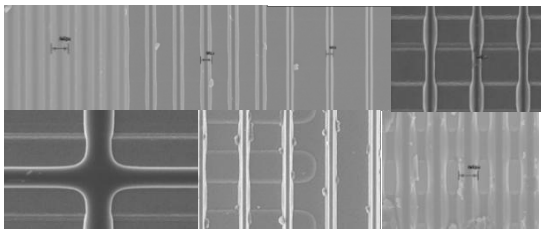

Figure 6. SEM picture of different stacked test keys

3. Simulation results and application examples

Based on optical method and mathematical method, OPC topography model can be established accurately, which can guide and modify the actual design. The main process of design is input design layout, corrected by OPC program, output OPC mask, and then checked by OPC verifies. Taking Poly film layer as an example in Figure 7, it can be seen that the design graphics recommended by OPC are all within the target. The actual shape of the image is more uniform than the traditional compensation method. The simulated contour of OPC model (green curve in the figure) almost coincides with the actual SEM.

Item	Design pattern	Actual pattern
Rule-based OPC		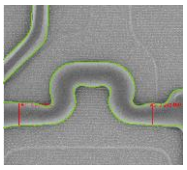
Model-based OPC		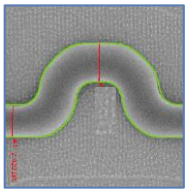

Figure 7. Rule-based and model-based simulation contour with actual SEM

In addition, model-based OPC simulation can predict process stability by adjusting exposure luminance, and improving CD uniformity by design. In Figure 8a, based on poly layer, we can see that in rule-based OPC simulation compensation, data with a CD range greater than 0.5um accounts for 93.75%. In Figure 8b, after model-based OPC simulation compensation, the data with CD range greater than 0.5um decreased to 25%. Model-based OPC simulation could improve CD fluctuation significantly.

(a)

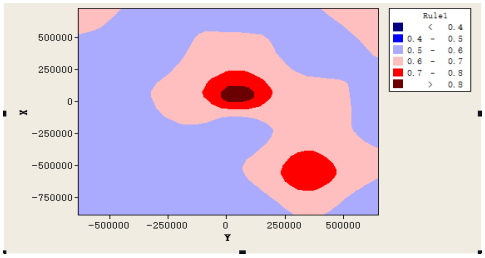

(b)

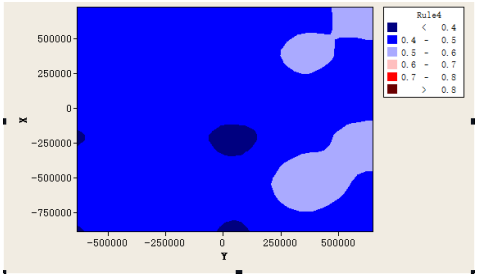

Figure 8. Rule-based OPC VS model-based OPC CD range

After optimizing the special problems of the panel substrate, the influence of the substrate can be accurately simulated in the new simulation model. As shown in Figure 9, the SEM image reveals an abnormal contour at the substrate boundary, and the OPC simulation (green line in the figure) accurately fit the topography changes with an error of < 0.1um.

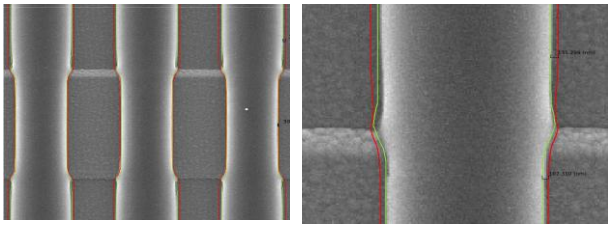

Figure 9. Simulation contour and actual pattern

OPC simulation can provide compensation based on the graphic density of different areas of the panel. Taking the MC layer as an example, the actual graphics accuracy of active area and different positions of fan-out is greatly improved after model-based OPC compensation. Model-based OPC deviation is smaller than 0.1um, and rule-based OPC deviation is about 0.4um.

Table 4. Rule-based compensation

Item(unit um)	target	DOG	gap
Active area	2	2.07	-0.07
Fanout2	2	1.76	0.24
Fanout1	3.2	2.80	0.4

Table 5. Model-based simulation

Item(unit um)	target	DOG	GAP
Fanout1	2.5	2.6	-0.1
	2.7	2.78	-0.08
Fanout2	2	2.07	-0.07
	2.2	2.27	-0.07
	5	4.96	0.04
AA hole	4.08	4.18	-0.1
	2.6	2.7	-0.1
Active area	2.38	2.47	-0.09
	1.7	1.7	0

4. Conclusion

In summary, we have developed a novel simulation method based on computer calculation and big data modeling on the panels, which solves the problems of lag and poor variability in traditional modes effectively. Meanwhile, the costs of time and fee can be reduced owing to avoiding the modifications of photo masks after design outsourcing. Especially, through OPC simulation, it is possible to achieve an error of less than 100nm for the multi-layer metal stacking structure and different graphic densities of LTPO products. In future, we believe that this method provides important technical guidance for the design of higher PPI products and other more complex technologies.

5. References

1. W. Otto, J. G. Garofalo, K. K. Low, C. M. Yuan, C. Pierrat, R. L. Kostelak, S. Vaidya and P. K. Vasudev: Proc. SPIE Vol. 2197 (1994) 278.
2. T. Kotani, S. Kobayashi, H. Ichikawa; S. Tanaka, S. Watanabe and S. Inoue: Proc. SPIE Vol. 4691 (2002) 188-195
3. M. L. Rieger and J. P. Stirniman: Proc. SPIE Vol. 2197 (1994) 371.
4. J. Zhao, J. Garofaro, J. Blatchford, E. Ehrlacher and E. Nease: Proc. SPIE Vol. 3334 (1998) 234.
5. C. A. Spence, J. L. Nistler, E. Barouch, U. Hollerbach and S. A. Orszac: Proc. SPIE Vol. 2197 (1994) 302.
6. S. Ram, E. S.Ward and R. J. Ober: Proceedings of the National Academy of Sciences of the United States of America. 103(12) (2006) 4457-4462.
7. L. Dong, Y. Li, X. Guo, H. Liu, and K. Liu: OPTICAL REVIEW Vol. 21, No. 3 (2014) 270–275.
8. M. Totzeck, J. Ruoff, D. Flagello, P. Gräupner, T. Heil, A.Göhnermeier, O. Dittmann, D. Krähmer, and V. Kamenov: J. Micro/Nanolithogr. MEMS MOEMS 4 [3] (2005) 031108.